



New viral sequences and endogenous viral elements (EVE) in world-wide populations of *Trioza erytreae*, the African citrus psyllid

Pedro Serra^{a,*}, Javier Forment^a, Michela Chiumenti^b, Alberto Fereres^c, José Alberto Pereira^d, Hans J. Maree^{e,f}, Rachelle Bester^{e,f}, Bernard Reynaud^{g,h}, Hélène Delatte^g, Leandro Peña^a, Marcos de la Peña^a, Beatriz Navarro^b, Francesco Di Serio^b, Ricardo Flores^{a,1}, Vicente Pallás^{a,1}

^a Institute of Molecular and Cellular Biology of Plants, Universitat Politècnica de València -Spanish National Research Council (CSIC), Valencia, Spain

^b Institute for Sustainable Plant Protection, National Research Council, Bari, Italy

^c Spanish National Research Council, Madrid, Spain

^d CIMO, SusTEC, Instituto Politécnico de Bragança, Campus Sta Apolónia, 5300-253, Bragança, Portugal

^e Department of Genetics, Stellenbosch University, Stellenbosch, South Africa

^f Citrus Research International, Stellenbosch, South Africa

^g Université de La Réunion, UMR PVBMT, F-97410 Saint Pierre, La Réunion, France

^h CIRAD, UMR PVBMT, F-97410 St Pierre, La Réunion, France

ARTICLE INFO

Keywords:

HLB
Trioza erytreae
 Insect viruses
 EVEs
 Mycovirus
 siRNAs

ABSTRACT

The citrus industry is threatened by a devastating bacterial disease known as Huanglongbing (HLB) or citrus greening. Current control measures largely rely on chemical suppression of insect vectors, primarily *Diaphorina citri* and *Trioza erytreae*. A promising alternative lies in the biotechnological use of viruses that specifically infect these vectors. Although much progress has been made in elucidating the virome of *D. citri*, there is no data on the viral population that *Trioza erytreae* can harbor and/or infect it. In this study, we analyzed the virome of *T. erytreae* from the Iberian Peninsula, Madeira, the Canary Islands, São Tomé and Príncipe, the Reunion Islands, and South Africa. We identified seven new insect-specific viruses (ISV) belonging to the families *Narnaviridae*, *Totiviridae*, *Solemoviridae*, *Phenuiviridae*, *Flaviviridae*, and *Tombusviridae*, the last three detected only in South African populations, four mycoviruses of the *Ambiguiviridae*, *Botourmiaviridae*, and *Partitiviridae* families, and three viruses known to infect citrus. Furthermore, comparison with the DNA sequence database has allowed us to identify the presence of 22 actively expressed endogenous viral elements (EVEs; virus-derived genetic material integrated into the genome of a nonviral host). Our findings provide new insights into the virome of this important insect vector and new perspectives to its potential for biocontrol strategies against HLB.

1. Introduction

Huanglongbing (HLB), considered the major threat to the world citrus industry (Bové, 2006), is an insect-vector-borne bacterial disease of citrus, involving three closely related phloem-restricted Gram-negative bacterial species: ‘*Candidatus Liberibacter asiaticus*’ (CLAs), ‘*Ca. Lepus americanus*’ (CLam) and ‘*Ca. L. africanus*’ (CLaf). CLAs and CLam are naturally transmitted by the Asian citrus psyllid *Diaphorina citri* (ACP) and CLaf by the African citrus psyllid *Trioza erytreae* (AfCP) (reviewed by Wang et al., 2017). HLB pathogens and insect vectors are widespread

worldwide, drastically reducing citrus production in areas where they are established. Among them, CLAs and ACP are the most widely distributed and have been reported in Asia, North America, South America, Oceania and Africa while CLam, originally identified in Brazil, is being competed by CLAs (de Godoy Gasparoto et al., 2022). CLaf and AfCP are present in Africa and Arabian Peninsula (da Graça et al., 2016, 2022; EPPO, 2025). As far as the European territory is concerned HLB has a serious impact on the French West Indies and Réunion but it is still absent from the Mediterranean basin and continental Europe. However, *D. citri* has been recently found in Israel and Cyprus (EPPO, 2025) and

* Corresponding author.

E-mail addresses: pedseral@upvnet.upv.es (P. Serra), vpallas@ibmcp.upv.es (V. Pallás).

¹ Deceased. This work is dedicated to the memory of Professor Ricardo Flores, who began coordinating this study.

T. erythrae has been detected in Madeira (Carvalho and Aguilar, 1997), Canary Islands (González-Hernández, 2003). In the last decade the vector has been introduced in the Iberian Peninsula, where it has colonized the Cantabrian and Atlantic coasts (Pérez-Otero et al., 2015; Arenas-Arenas et al., 2018, 2019) thus posing a major threat to the Spanish citriculture, the largest citrus producer in Europe. Recent results suggest that the outbreaks of *T. erythrae* in the Iberian Peninsula may have derived from the Canary Islands (Ruíz-Rivero et al., 2021; Chiumenti et al., 2025). The populations of *T. erythrae* that invaded Macaronesia (Madeira and the Canary Islands) and the Iberian Peninsula are likely to have originated from southern Africa (Ruíz-Rivero et al., 2021; Chiumenti et al., 2025). *T. erythrae* has been shown to be an efficient vector of CLAs being able to efficiently transmit the bacteria to seedlings at a similar rate than *D. citri* highlighting the high risk of spread of the most aggressive variant of HLB (CLAs) by *T. erythrae* in Europe (Reynaud et al., 2022).

Since HLB has no cure, the control and containment of this disease is approached with a combination of multidisciplinary strategies for which the management of insect vectors by chemical and biological methods is of special relevance (Alquézar et al., 2022). In this regard, the use of viruses affecting insects as biological control agents can be a tool to help us reduce vector populations (Nouri et al., 2018). Although insects are the most extensive and varied class in the animal kingdom, the knowledge about the viruses that infect them is scarce compared to viruses that affect bacteria, plants or vertebrates. Many of the studies have focused on blood-sucking insects that transmit diseases to humans and animals. The rise of high-throughput sequencing technologies and bioinformatics technologies, however, has allowed in the last decade to expand the knowledge about viruses of insects relevant to agriculture. With respect to psyllid vectors of HLB, emphasis has been placed on *D. citri* with some metagenomic studies that have identified DNA and RNA viruses (Nouri et al., 2016; Britt et al., 2020; Chen et al., 2020; Nigg et al., 2020; Rashidi et al., 2022; Lin et al., 2023) including Diaphorina citri-associated C virus (DcACV), Diaphorina citri densovirus (DcDV), Diaphorina citri flavivirus-like virus (DcFLV), Diaphorina citri picorna-like virus (DcPLV), Diaphorina citri reovirus (DcRV) and *D. citri* cimodo-like virus, DcCLV, from the families *Parvoviridae*, *Flaviviridae*, *Iflaviridae*, *Reoviridae*, and an unclassified (+) ssRNA virus. Remarkably, recent results showed that *D. citri* vectors with DcFLV exhibit greater CLAs transmission efficiency than those without virus (Lin et al., 2025; Galdeano et al., 2025) suggesting the possibility of manipulating DcFLV in *D. citri* populations to reduce CLAs transmission for HLB disease management. A recent study of *D. citri* samples from two islands in Samoa has identified 11 candidates for new viruses belonging to the families *Yadokariviridae*, *Botourmiaviridae*, *Nodaviridae*, *Mymonaviridae*, *Partitiviridae*, *Totiviridae*, and *Polymycoviridae* (Etebari et al., 2025). In addition, a new genus, “*Psyllodivirus*”, has been recently proposed to accommodate the distinctive features, such as such as an inverted protein order and a novel IRES, that 13 Chinese isolates of DcPLV present in their genomic organization (Du et al., 2026). Recently, Britt-Ugarte-mendia et al. (2025) discovered the eighth Asian citrus psyllid-associated viral sequence, tentatively called Diaphorina citri virga-like virus (DcVLV) since its sequence is similar to other unassigned viruses discovered in insects, specifically of the family *Virgaviridae*. In the case of *T. erythrae*, no study to date has addressed the identification of viruses that affect them.

In this work we report the first catalog of viruses that infect populations of *T. erythrae* collected in different geographical areas with special attention to those that are invading the Iberian Peninsula. The identification and characterization of viruses has been carried out by a metagenomics approach using DNA, RNA and siRNA high-throughput sequencing.

2. Methodology

2.1. Sample collection

We have selected locations along the Cantabrian and Atlantic coast of the Iberian Peninsula being two locations in Portugal (Vairao and Mafra) and five in Spain (O Grove in Galicia, Navia in Asturias, Cobrecos and La Helguera in Cantabria and Deusto in Basque country). We have also selected three samples belonging to Atlantic Island territories of Madeira (A Poncha de Fatima), Canary Islands (Tenerife) and São Tomé and Príncipe (Santa Lúzia) which is located in East Africa and one from Reunion Island located in the southwest African side of the Indian ocean. In addition, three locations in South Africa have also been included: Gqeberha (former Port Elizabeth; in the figures and tables the abbreviation PE has been used to refer to this location since the samples are the same as those used in the work of Chiumenti et al. (2025), where the name of the city had not been changed yet), Stellenbosch and Buffeljagsrivier (Fig. S1).

Adults of *T. erythrae* (males and females) were collected in citrus fields, washed with PBS and submerged in RNAlater Stabilization Solution (Invitrogen). Samples were kept at 4 °C during transport and storage. Following receipt of the samples, RNA extracts were obtained from a pool of five insects sampled from each location under study using RNeasy® Lipid Tissue (Qiagen) and with TRIzol™ Reagent (Thermo-fisher scientific) for samples from South Africa.

2.2. High-throughput sequencing

RNA extracts were previously subjected to a rRNA depletion of both the insects and prokaryotes using RiboZero human/mouse/rat and RiboZero microbiology Kits (Illumina). Once a high-quality total RNA preparation was obtained, an aliquot was used to generate a TruSeq stranded Total RNA library (Illumina) and sequenced in 150 paired-end (PE) format using Illumina platform to obtain around 50 million sequence pairs (per sample). A second aliquot was used to generate small RNA (sRNA) libraries by using the TruSeq small RNA Library prep kit (Illumina), that were sequenced on the Novaseq/Nextseq Illumina platforms, in a 75 single read (SR) format to obtain around 50 million raw sequences (per library).

2.3. Contig assembly

Adaptor removal and quality-trimming of raw reads were done with cutadapt (<https://doi.org/10.14806/ej.17.1.200>). Clean reads were quality assessed using FastQC (<https://www.bioinformatics.babraham.ac.uk/projects/fastqc/>) and assembled with SPAdes (<https://doi.org/10.1002/cpb.102>) using the mvavial assembly mode with a multiple k-mer approach (41, 51, 61, 71, 81, 91, 101, 111, 121).

2.4. Identification of viral sequences

The resulting contigs were compared against the nonredundant viral protein database available in NCBI using BLASTX. From the approximately 14,000 contigs per sample obtained, only those for which sequence homology (E-value equal to or less than 10^{-4}) to RNA dependent RNA polymerases (RdRp), glycoproteins, capsid proteins and nucleoproteins that have no homology with non-viral organisms (with the exception of some sporadic sequences from metagenomic studies of insects without well-defined annotation) were selected. Alternatively, the resulting contigs were analysed with the palmscan algorithm (<https://github.com/rcedgar/palmscan>). This software allows the detection of viral RdRp through the identification of the A, B and C motifs conserved in the palm domains of known RdRps (Edgar et al., 2022). Results were then inspected manually to screen for potential viral sequences. Additionally, searches for viroid-like sequences (viroids and viral RNA satellites with circular RNA genomes) were performed

through the identification of potentially circular RNA contigs resulting from the assemblies (Forgia et al., 2023). The presence of self-cleaving ribozymes was investigated through the INFERNAL software, an algorithm for identifying RNA elements using secondary structure and nucleotide covariation modelling (Nawrocki and Eddy, 2013). The scaffolds in which viral sequences have been identified were subjected to Blastn on DNA-seq libraries constructed from insect samples collected from the same trees and on the same dates (Chiumenti et al., 2025). Using DNA-seq, the size of the scaffolds that showed total homology were expanded.

2.5. sRNA mapping

Adaptor removal and quality-trimming of sRNA raw reads, as well as a selection of the 15–35 nt resulting reads, was done with cutadapt (<https://doi.org/10.14806/ej.17.1.200>). Clean, 15–35 nt reads from each sample were mapped to each of the forward and reverse sequences of the selected viral sequences using HISAT2 (<https://www.nature.com/articles/s41587-019-0201-4>). To get the size distribution and other statistics of the reads mapping to the virus sequences, FastQC (<http://www.bioinformatics.babraham.ac.uk/projects/fastqc/>) was used. In the case of scaffold 36, the mapping of forward sRNAs was performed by removing a sequence fragment (from 1 to 303 nts) due to its high homology with 28S ribosomal RNA gene of the insect, which caused an alteration in the results.

2.6. RNA-seq mapping

Cleaned RNA-Seq data for the two samples (SAMN49798504_São Tomé and SAMN49798502_Gqeberha) that contain all the viral sequences identified in this work were first mapped with 'bwa mem' against each of the selected viruses from its location (São Tomé and Príncipe and South Africa, respectively) and only unique mappings were conserved using samtools (Li and Durbin, 2010; Danecek et al., 2021). Clean reads were also independently mapped with 'bwa mem' against an artificial genome created by combining the insect genome and each selected virus. Only unique read mappings were conserved using samtools. Mappings specific to the virus genome were then selected with samtools..

Based on the RNA-seq mappings, reads corresponding to scaffolds containing viral sequences were quantified and their positions determined. Coverage plots were generated using Microsoft Excel. The RNA-seq alignments were further examined with IGV to assess nucleotide variability within the viral sequences at their initial detection sites. At each position, only sequence variants present in more than 20 % of the reads were considered.

2.7. Viral characterization

Proteins encoded by the viral sequences were predicted and annotated using ExPASy Translate (Duvaud et al., 2021). Open reading frames (ORFs) were functionally characterized through BLASTp searches against the NCBI viral database. After identifying the RNA-dependent RNA polymerase (RdRp) of each novel virus candidate, phylogenetic analyses were conducted using the 50 RdRp sequences with the highest identity retrieved from the NCBI database. Multiple sequence alignments were generated with MAFFT v7 (Katoh et al., 2019). Phylogenetic trees were reconstructed using the neighbor-joining method with 1000 bootstrap replicates and visualized with Archaeopteryx.js (Han and Zmasek, 2009). Percent identity matrices and phylogenetic trees for RdRps from virus-like strains detected at different locations were generated using the EMBL-EBI Job Dispatcher sequence analysis framework (Madeira et al., 2024).

3. Results

3.1. Viral sequence characterization

14 TruSeq stranded RNA libraries, yielding approximately 50 million PE reads per sample, were generated from RNA from five insects per location. The list and the statistical values of the assembled RNA-seq contigs of the *T. erythrae* from each of the different locations are summarized in Table S1.

Viral sequences were identified using two complementary approaches: (i) sequence homology searches against NCBI viral and non-redundant proteins databases using BLASTx, focusing on those corresponding to RdRps, glycoproteins, capsid proteins and nucleoproteins, and (ii) detection of conserved RdRp motifs using the Palmscan algorithm.

We also leveraged the availability of DNA-seq datasets described in Chiumenti et al. (2025), generated from the same *T. erythrae* populations (insects collected from the same trees at the same time) used for RNA-seq. This enabled verification of whether viral sequences identified in RNA-seq were also present in DNA form by performing BLASTn searches against the DNA-seq datasets from the same populations. Using this approach, we identified novel viral sequences with homology to known viruses from multiple genera (Table S2; sequences provided in the Additional File), which can be divided into two groups. One group (scaffolds 1–22 in Table S2) consists of sequences belonging to the families *Chuviridae*, *Xinmoviridae*, *Sedoreoviridae*, *Orthomyxoviridae*, *Partitiviridae* (RNA viruses) and *Parvoviridae* (DNA virus) that have been detected in both DNA-seq and RNA-seq datasets from almost all locations. This is surprising, since with the exception of the last family, *Parvoviridae*, the rest of the sequences belong to the kingdom Orthornavirae (RNA viruses with RdRp). In a second group (scaffolds 23 to 39 in Table S2), viral sequences were only detected in the RNA-seq datasets and share homology to known RNA viruses of the families *Totiviridae*, *Ambiguiviridae*, *Botourmiaviridae* and *Partitiviridae* (detected only in samples from São Tomé and Príncipe), *Solemoviridae* (in samples from São Tomé and Príncipe, Reunion Island and the three South African locations), *Phenuiviridae*, *Flaviviridae* and *Tombusviridae* (in samples from at least one South African population) and *Narnaviridae* (in samples from all the locations studied except for those coming from Réunion island).

Citrus viruses, among which are citrus vein enation virus, citrus tristeza virus (CTV) and citrus virus A, were also identified in insects from different geographical areas (Table S3), but this is likely detections from the remains in the mouth and stomach apparatus of the *T. erythrae* last ingestions before being collected, highlighting the power of the sequencing method used.

3.2. sRNAs mappings help to determine the nature of the viral sequences identified

To delve deeper into the nature of these viral sequences, three sRNA libraries were generated from RNA extracts of insects from populations in La Helguera (Spain), São Tomé and Príncipe and Gqeberha (South Africa). These samples were selected because all identified viral sequences were detected in at least one of them. Scaffolds containing viral sequences were subjected to sRNA read mapping. The results, summarized in Table S4, reveal clear differences between sequences detected in both RNA-seq and DNA-seq datasets across most locations (group I) and those detected only in RNA-seq datasets from some locations (group II). sRNA mappings on scaffolds belonging to group I (Fig. 1, Fig. S2 and Table S4 colored in blue) show a predominant size around 30 nts. Moreover, sRNAs of at least one of the polarities (which coincides with the most abundant siRNA count) predominantly carry a 5' uracil. These features are characteristic of the PIWI-interacting RNAs (piRNAs), which function as small guide RNAs to repress transposon expression in animals and described as a antiviral defense mechanism in insects (Nouri et al., 2018). Because piRNAs can derive from endogenous viral

elements (EVEs), we interpret that the viral sequences in these scaffolds (1–22), detected in both DNA-seq and RNA-seq datasets, do not represent active viral infections but rather EVEs integrated into the *T. erythrae* genome (see Discussion section).

In contrast to group I, sRNA mapping to group II scaffolds (Fig. 1, Fig. S3 and Table S4, colored in orange) displayed features consistent with post-transcriptional gene silencing (PTGS), including siRNAs of 21–23 nt with a symmetric strand distribution. These characteristics suggest the corresponding contigs derived from active viral infections. Within this group II, two subgroups can be considered: i) IIa (dark orange in Table S4, scaffolds 23–33 in Fig. S2) characterized by a predominant size of 21 nt and no nucleotide preference at the 5' end and ii) subgroup IIb (light orange in Table S4, scaffolds 34–39 in Fig. S3) with a size of 22–23 nt and preference for uracil at their 5' ends, features that are characteristics of sRNAs derived from viruses infecting fungi (Wang et al., 2016; Donaire and Ayllon, 2017; Wang et al., 2019; Pang et al., 2022). Consistently, all the scaffolds of group IIa are related to insect-specific viruses whereas those of subgroup IIb are referred by BLAST analysis to sequences from mycoviruses that are infecting fungi from the insect's microbiota and are therefore associated with *T. erythrae*. To support this hypothesis, we searched for fungal signatures in the RNA-seq of insects from São Tomé and Príncipe, where the putative mycovirus were detected. We identified the three nuclear ribosomal markers commonly used for fungal identification (ITS, LSU and SSU), as well as the mitochondrial cytochrome c oxidase gene (COX1) (Tekpinar and Kalmer, 2019). Additional File 2 presents two representative sequences of each marker, and Table S5 summarizes the BLASTn results against the NCBI database (see below for description of the viruses).

To validate group II scaffolds, RNA-seq reads-after removing sequences also present in DNA-seq datasets to exclude transcripts encoded in the insect genome-were mapped back to these scaffolds, and read depth across assemblies was assessed. Coverage profiles for all group II scaffolds are shown in Fig. S4. By grouping these scaffolds by virus family and comparing them with the known viruses with the closest homologs, we reconstructed genome organization and annotated ORFs for the putative novel viruses. Classification was based on phylogenetic analyses of RdRp sequences, including the 50 closest homologs identified by BLASTp against NCBI protein databases (Fig. S5). A summary of the putative novel viruses is provided in Table 1 and Fig. 2.

3.3. Insect-specific viruses

We identified seven new viruses infecting *T. erythrae*. It must be taken into account that since these viruses were only detected by bioinformatics in HTS data and no additional validations were conducted, the genome sizes are approximate and 'complete genomes' refer to genomes where all the ORFs are complete. A putative new narnavirus-like was detected, *Triozia erythrae* narna-like virus (TeNLV), with a monopartite ssRNA(+) and a genome size of 3272 nt (Fig. 2A, upper). Like a subset of narnaviruses called "ambigrammatic", TeNLV exhibits overlapping ORFs on opposite strands: the positive strand encodes a 1065 aa RdRp, and the negative strand encodes a 1054 aa hypothetical protein. The TeNLV infection in samples from São Tomé and Príncipe shows a variability of 46 nucleotide changes, and the aa variability of its RdRp indicates differences between European and South African sequences and the one detected in São Tomé and Príncipe, which is more closely related to the one detected in Gqeberha (formerly Port Elizabeth) (Fig. S6). Narnaviruses have been detected in fungi, plants, protists, and arthropods, including insects (Göertz et al., 2019). TeNLV shares highest BLASTx similarity (44.74 %) with Hubei narna-like virus 21 and was detected in all populations except Réunion Island, indicating the widespread distribution of this virus-like. A novel totivirus-like, tentatively named *Triozia erythrae* toti-like virus (TeTLV), was identified as a monopartite dsRNA virus with a 5220 nt genome encoding a 794 aa coat protein overlapping, in a different reading frame, a 926 aa RdRp (Fig. 2.

A, middle). Initially, totiviruses were only known to infect fungi and other eukaryotes, as well as plants, but recently they have been detected in insects and bats (Couto et al., 2024; Leal et al., 2023). TeTLV RdRp shares highest BLASTx similarity (41.24 %) with solenopsis midden virus, a totivirus detected in fire ants (Valles and Rivers, 2019) and the CP with *Hermetia illucens* toti-like virus 1 (26,11 %). TeTLV has been detected in the São Tomé and Príncipe population with a variability of 42 nucleotide substitutions. A new putative sobemovirus, *Triozia erythrae* sobemo-like virus (TeSLV), with a bisegmented ssRNA(+) genome harboring a 2807 nt RNA 1 encoding a 484 aa hypothetical protein and a 926 aa RdRp, and a 1874 nt RNA 2 encoding a 223 aa capsid protein and a 247 aa hypothetical protein (Fig. 2A, lower). Sobemoviruses were considered a group of plant viruses with non-segmented ssRNA(+) genomes approximately 4 kb in length. However, subsequent studies have described new sobemoviruses detected in invertebrates classified in a new phylogenetically divergent but related clade that includes both viruses with mono- and bisegmented genomes (Shi et al., 2016). The RdRp of TeSLV has highest sequence homology (48 %) with *Atrato sobemo*-like viruses 1 and the CP with the *Atrato sobemo*-like viruses 2 (38,51 %). Both viruses were detected in mosquitoes and, like other viruses described in other arthropods such as centipedes, share the same genomic organization as TeSLV. We detected this new virus in populations from Réunion Island, the three locations in South Africa studied, and São Tomé and Príncipe, where a variability of 233 nucleotide substitutions in RNA1 and 20 in RNA2, was observed. The aa sequences of RdRp indicate a relationship between the Gqeberha and Reunion variants, which are close to that of São Tomé and Príncipe, and, at a greater phylogenetic distance, those of Stellenbosch and Buffeljagsrivier (Fig. S6).

Four additional putative viruses were detected exclusively in South African populations (Fig. 2B). This includes a putative virus belonging *Phenuiviridae* family, *Triozia erythrae* phenui-like virus (TePLV), with a trisegmented ssRNA(-) genome composed of a 6520 nt long L segment encodes an RdRp of 2123 aa; an M segment encodes a 987 aa polyprotein with the highest aa identity to the RdRp (30,82 %) and the glycoprotein (25,67 %) of Dar es Salaam virus, and a 1004 nt S segment encoding a 248 aa protein with the highest sequence identity (30,15 %) with the nucleocapsid protein of Hymenopteran phenui-related virus. TePLV has only been detected in Gqeberha with very low nucleotide variability: 5 substitutions in segment L, 3 in segment M, and 1 in segment S. A new putative flavivirus, *Tryozia erythrae* flavi-like virus (TeFLV), was detected in Gqeberha and Stellenbosch. It possesses a 19,250 nt positive-sense ssRNA genome encoding a large polyprotein of 6169 aa with the highest aa identity (33,25 %) with that of *Macrosiphum euphorbiae* virus 1. The Gqeberha samples showed sequence variability of 292 nucleotide substitutions and an aa difference of 99.43 % compared to the Stellenbosch variant. The other two viruses only detected in the South African populations includes two new putative tobusviruses with different genomic organizations: i) *Triozia erythrae* tobus-like virus 1 (TeToLV1), detected in all South African locations studied, of the monopartite ssRNA(+) category, has a 2276 nt genome encoding a 262 aa hypothetical protein that overlaps the sequence in another reading frame of a 483 aa RdRp with high sequence identity (42,07 %) to that of Dipteran tobus-related virus and ii) *Triozia erythrae* tobus-like virus 2 (TeToLV2), a bisegmented ssRNA(+) virus with a segment 1 of 2523 nt encoding a hypothetical protein of 319 aa whose sequence overlaps in another reading frame with that of a 494 aa RdRp. This RdRp has 62,55 % of identity with the RNA 1-encoded protein of *Diaphorina citri* associated C virus. Segment 2 has a size of 1751 nt that encodes a hypothetical protein of 163 aa whose sequence end overlaps in another reading frame with the beginning of another hypothetical protein of 434 aa with high sequence identity (28,22 %) to the putative virion glycoprotein of RNA 2 of *Diaphorina citri* associated C virus. TeToLV1 shows a single nucleotide substitution and TeToLV2 shows 36 in RNA1 and 17 in RNA2 in samples from Gqeberha. The aa sequences of the RdRp indicate a greater phylogenetic distance in

Table 1
Putative new viruses identified in *T. erytrae*.

Tentative name for putative virus	Scaffold number	Virus category	Acronym	Largest sequence length (nts) obtained	Encoded protein	Genome position	Accession	Closest relative virus (BLASTx)	Tentative virus family or superfamily	Source of <i>T. erytrae</i> populations
Insect specific viruses										
Trioza erytrae narna-like virus	23	ssRNA (+)	TeNLV	3272	RdRP HyP	4 to 3198 3231 to 67	PV844715 XXH82223 XXH82224 PV844716	Hubei narna-like virus 21	<i>Narnaviridae</i>	All except REU
Trioza erytrae toti-like virus	24	dsRNA	TeTLV	5220	CP RdRP	173 to 2557 2146..4926	XXH82225 XXH82226 PV844717	Solenopsis midden virus	<i>Totiviridae</i>	SAO
Trioza erytrae sobemo-like virus	25	ssRNA (+)	TeSLV	RNA 1.: 2807	HyP RdRP	72 to 1526 1616 to 2761	XXH82227 XXH82228 PV844718	Atrato Sobemo-like virus 1	<i>Solemoviridae</i>	SAO, REU, PE, BJ, STER
	26			RNA 2.: 1874	CP HyP	77 to 748 872 to 1615	XXH82229 XXH82230 PV844719	Atrato Sobemo-like virus 2		
Trioza erytrae phenui-like virus	27	ssRNA(-)	TePLV	Seg L: 6520	RdRP	6443 to 72	XXH82231 PV844720	Dar es Salaam virus	<i>Phenuiviridae</i>	PE
	28			Seg M: 3240	PolyP	3132 to 169	XXH82232 PV844721	Dar es Salaam virus		
	29			Seg S.: 1004	NP	938 to 192	XXH82233 PV844722	Hymenopteran phenui-related virus		
Trioza erytrae flavi-like virus	30	ssRNA (+)	TeFLV	19,250	PolyP	285 to 18,794	XXH82234 PV844723	Macrosiphum euphorbiae virus 1	<i>Flaviviridae</i>	PE, STER
Trioza erytrae tombus-like virus 1	31	ssRNA (+)	TeToLV1	2276	HyP RdRP	33 to 821 725 to 2176	XXH82235 XXH82236 PV844724	Dipteran tombus-related virus	<i>Tombusviridae</i>	PE, BJ, STER
Trioza erytrae tombus-like virus 2	32	ssRNA (+)	TeToLV2	RNA 1.: 2523	HyP RdRP	157 to 1116 741 to 2225	XXH82237 XXH82238 PV844725	Diaphorina citri associated C virus	<i>Tombusviridae</i>	PE, BJ, STER
	33			RNA 2.: 1751	HyP HyP	91 to 585 294 to 1598	XXH82239 XXH82240	Diaphorina citri associated C virus		
Putative mycoviruses										
Trioza erytrae associated ambigivirus	34	ssRNA (+)	TeAAV	3348	HyP RdRP	32 to 931 1046 to 2503	PV844726 XXH82241 XXH82242	Erysiphe necator associated ambigivirus 2	<i>Ambiguviridae</i>	SAO
Trioza erytrae associated botourmiavirus	35	ssRNA (+)	TeABV	1691 (partial)	RdRP	50 to 1691 (partial)	PV844731 XXH82247	Magnaporthe oryzae botourmiavirus 2	<i>Botourmiaviridae</i>	SAO
Trioza erytrae associated partitivirus 1	36	dsRNA	TeAPV1	RNA 1.: 2064	RdRP	64 to 1889	PV844727 XXH82243 PV844728	Sarcosphaera coronaria partitivirus	<i>Partitiviridae</i>	SAO
	37			RNA 2.: 1846	CP	78 to 1698	XXH82244	Clohesyomyces aquaticus partitivirus 1		

(continued on next page)

Table 1 (continued)

Tentative name for putative virus	Scaffold number	Virus category	Acronym	Largest sequence length (nts) obtained	Encoded protein	Genome position	Accession	Closest relative virus (BLASTx)	Tentative virus family or superfamily	Source of <i>T. erythrae</i> populations
Trioza erythrae associated partitivirus 2	38	dsRNA	TeAPV2	RNA 1.: 1702			PV844729	Beauveria bassiana partitivirus 4	<i>Partitiviridae</i>	SAO
	39			RNA 2.: 1552	RdRp	37 to 1656	XXH82245 PV844730	Beauveria bassiana partitivirus 4		
					CP	43 to 1367	XXH82246			

*Seg., Segment; RdRp, RNA-dependent RNA polymerase; HyP, hypothetical protein; CP, capsid protein; PolyP, polyprotein; NP, nucleoprotein ALL, all locations; REU, Reunion Island; SAO, São Tomé and Príncipe; PE, Gqeberha formerly Port Elizabeth; BJ, Buffeljagsrivier; STER, Stellenbosch.

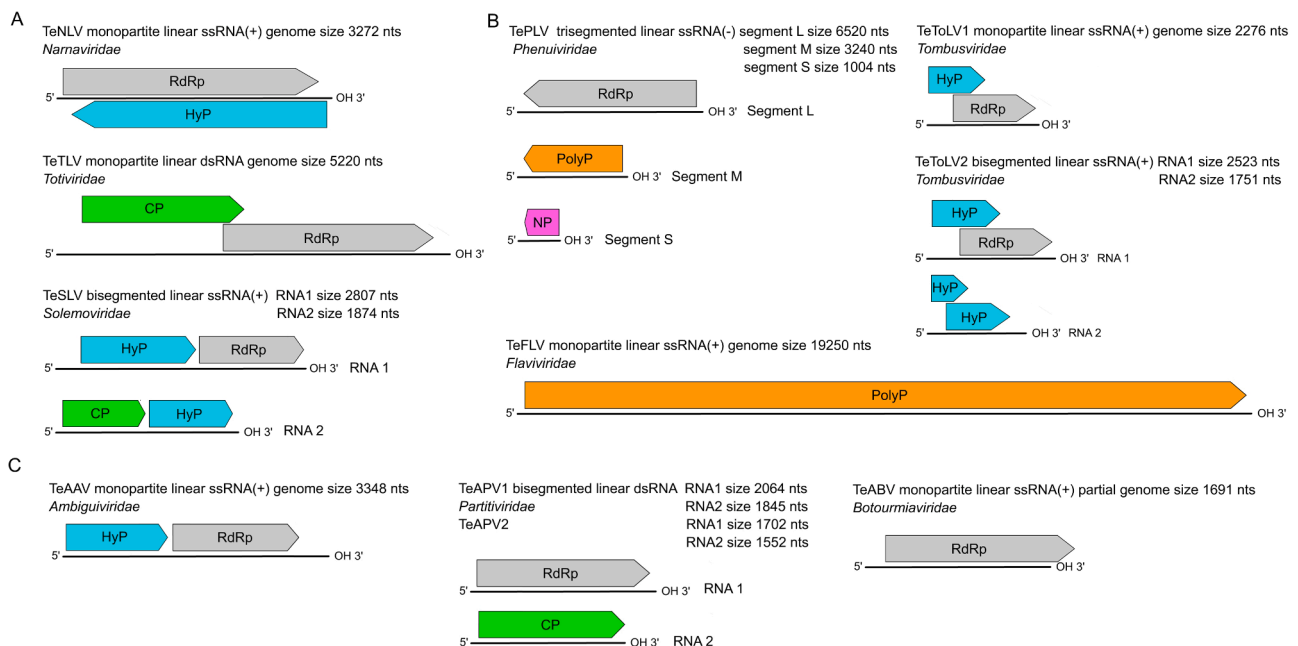


Fig. 2. genome organization of insect specific virus-like A: detected in São Tomé and Príncipe. B: detected exclusively in South Africa and C: mycovirus associated to *T. erythrae* detected in São Tomé and Príncipe. *TeNLV, *Trioza erythrae* narna-like virus; TeTLV, *Trioza erythrae* toti-like virus; TeSLV, *Trioza erythrae* sobemo-like virus; TePLV, *Trioza erythrae* phenui-like virus; TeFLV, *Trioza erythrae* flavi-like virus; TeToLV1, *Trioza erythrae* tobus-like virus 1; TeToV2, *Trioza erythrae* tobus-like virus 2; TeAAV, *Trioza erythrae* associated ambiguiivirus; TeAPV1, *Trioza erythrae* associated partitivirus 1; TeAPV2, *Trioza erythrae* associated partitivirus 2; TeABV, *Trioza erythrae* associated botourmiavirus. RdRp, RNA-dependent RNA polymerase; HyP, hypothetical protein; CP, capsid protein; PolyP, polyprotein; NP, nucleoprotein.

samples from this location compared to those from Stellenbosch and Buffeljagsrivier for both virus-like. Although tobusviruses were originally described as monopartite viruses that infect plants, numerous related viruses have recently been described in non-plant hosts, such as marine invertebrates and terrestrial arthropods, with both mono- and bisegmented genomic organizations (Shi et al., 2016). Our study provides a clear example of tobus-like viruses with both genome organizations.

3.4. Four new mycoviruses associated with *T. erythrae*

As described above, we identified viral sequences with characteristics consistent with the mycoviruses likely associated with *T. erythrae* (Fig. 2C) and that, consistently, they phylogenetically grouped among mycovirus sequences described in the datasets (Fig. S5). We identified a *Trioza erythrae* associated ambiguiivirus (TeAAV) of the ssRNA(+) category with a monopartite genome of 3348 nt (showing five nucleotide substitutions). The genome encodes a 299 aa hypothetical protein with high aa identity to that of grapevine wood holobiome associated ambiguiivirus 2 and, in the same reading frame, a 485 aa RdRp with the

highest aa identity (46,95 %) to the RdRp of *Erysiphe necator* associated ambiguiivirus 2 (Fig. 4, upper). "*Ambiguiviridae*" is a recently proposed family of viruses whose members lack a capsid protein and do not form true virions. As in other described ambiguiiviruses, TeAAV has a UAG stop codon at the end of ORF1 (Jia et al., 2023). Within the mycoviruses, we also identified two putative new partitiviruses belonging to the bisegmented dsRNA category (Fig. 2C, middle). *Trioza erythrae* associated partitivirus 1 (TeAPV1) has an RNA 1 of 2064 nt (with a variability of 6 nucleotide substitutions) encoding an RdRp of 608 aa with the highest aa identity (62,41 %) to the RdRp of *Sarcosphaera coronaria* partitivirus and an RNA 2 of 1845 nt (with a variability of 4 nucleotide substitutions) encoding a capsid protein of 540 aa with the highest aa identity (57,20 %) to that of *Clohesyomyces aquaticus* partitivirus 1. *Trioza erythrae* associated partitivirus 2 (TeAPV2) possesses a RNA1 of 1702 nt (with a variability of 1 nucleotide substitution) encoding an RdRp of 539 aa with the highest aa identity (72,46 %) to that of *Beauveria bassiana* partitivirus 4 and a RNA 2 of 1552 nt (with a variability of 1 nucleotide substitutions) which encodes a 441 aa capsid protein with the highest aa identity (60,05 %) to that of *Beauveria bassiana*

partitivirus 4. Finally, we obtained the partial sequence of a putative new mycovirus with a monopartite ssRNA(+) genome, likely a new member in the family *Botourmiaviridae* (Fig. 2C, lower) tentatively named *Trioza erytrae* associated botourmiavirus (TeABV). The identified sequence (1691 nt; five nucleotide substitutions) contains a partial ORF (lacking stop codon) encoding the N-terminal 547 aa of a putative protein, with the highest aa identity (63,85 %) with the RdRp to that of *Magnaporthe oryzae* botourmiavirus 2, which is a 607 aa long protein. Remarkably, all the mycoviruses identified in this study were detected only in the São Tomé and Príncipe sample.

4. Discussion

To date, continental Europe remains free from the devastating citrus disease HLB. However, populations of *T. erytrae*, a vector capable of transmitting all the bacterial species that cause HLB, are already established along the Atlantic and Cantabrian coasts of the Iberian Peninsula (Arenas-Arenas et al., 2018; Reynaud et al., 2022). This scenario raises a serious concern since the Mediterranean and southern regions of the Iberian Peninsula are major citrus production areas. The fight against HLB is multidisciplinary, and most studies on combating the vector have focused on *D. citri*, which has had the greatest impact worldwide, leaving *T. erytrae* comparatively understudied. Here, we compiled a virus catalog based on high-throughput sequencing (HTS) of whole-insect RNA extracts from *T. erytrae* populations collected across the Iberian Peninsula, European island territories, and African regions where the insect has been established for longer periods. Because the metagenomic approach includes microorganisms present in the digestive tract, virus detection does not necessarily indicate infection of the insect itself. This is exemplified by the detection of citrus-infecting viruses-citrus vein enation virus, citrus virus A, and citrus tristeza virus-, which most likely originated from plant material present in the mouthparts or digestive system following recent feeding. (Fig. 3, green color). It is important to note that the persistent presence of CTV infection in citrus throughout Florida groves has been reported (Britt

et al., 2020). In addition, it was demonstrated that CTV is transmitted by *D. citri* (Wu et al., 2021) and it seems to promote the acquisition and transmission of CLAs by *D. citri* (Chen et al., 2023). Britt-Ugartemendia et al. (2025), however, after comparing the presence or absence of CTV in different populations (laboratory-reared versus field) of ACPs, concluded that this important pathogen was only observed in field conditions, which suggests the origin of the CTV RNAs from a CTV-infected tree.

Using an HTS-based framework, we identified 22 putative new viral sequences integrated into the insect's genome, 19 of which were consistently detected across all sampled locations. EVEs represent genomic remnants of past infections that have been vertically inherited. The presence of scaffolds containing both viral sequences and transposon-associated proteins further supports an integration mechanism mediated by mobile genetic elements. Consistent with observations in *D. citri* and other insects, EVE-derived piRNAs may contribute to antiviral defense through sequence-specific silencing (ter Horst et al., 2019; Nigg et al., 2020; Cerqueira de Araujo et al., 2022). It is worth noting that the identified EVEs belong to six viral families: *Parvoviridae* ssDNA, *Chuviridae* ssRNA(-), *Xinmoviridae* ssRNA(-), *Sedoreoviridae* dsRNA, *Orthomyxoviridae* ssRNA(-), and *Partitiviridae* dsRNA, indicating that *T. erytrae* has suffered many of these events compared to those detected in other organisms. Our results are consistent with the available information (reviewed by Gilbert and Belliardo, 2022) indicating that the Hemiptera order, including *D. citri*, is one of those with the highest number of EVEs in its genome, with EVEs derived from viruses of the same families as those we have described in *T. erytrae* being particularly frequent. The viruses that integrated their sequences in *T. erytrae* are unknown, but the presence of these EVEs indicates the existence of several undescribed viruses belonging to different families that infect, or at least have infected, the insect. The fact that the majority of EVEs were detected in the genome of all the populations studied suggests that the integration events of these EVEs occurred in evolutionary history prior to the spread to the different locations studied.

In the *Trioza erytrae* virome, we identified 11 putative new viruses.

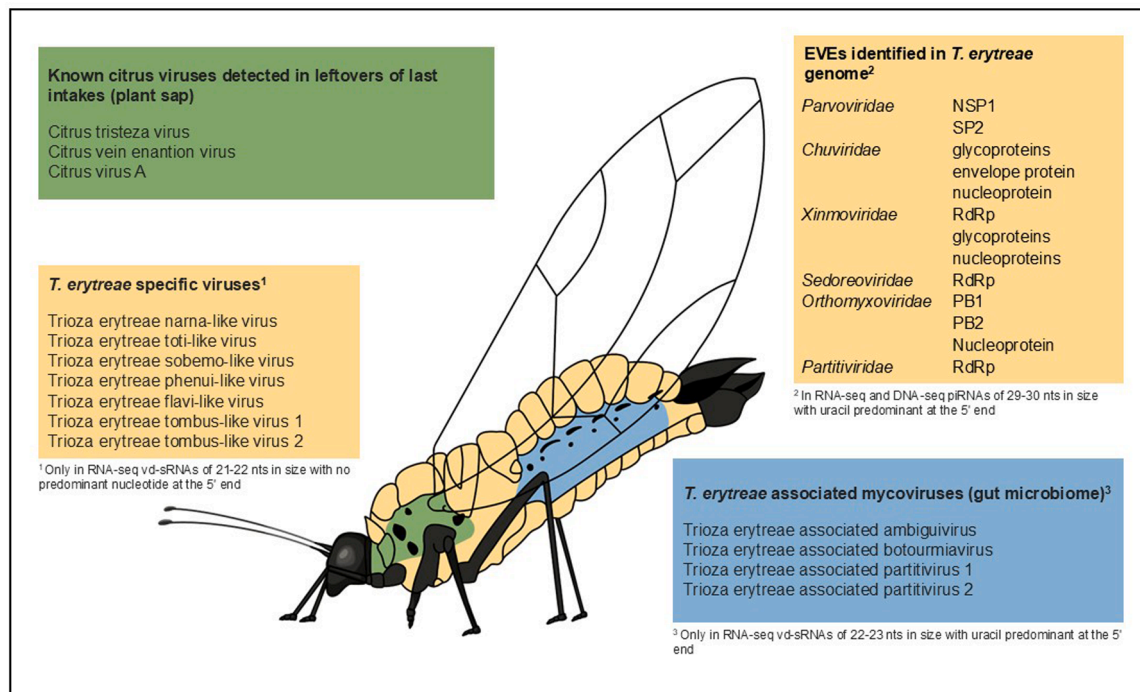


Fig. 3. Summary of the viral sequences identified in this study grouped by their characteristics. In the scheme of *T. erytrae* the colors indicate their possible localization in the insect but are not intended to reflect any tissue tropism: green, mouth and stomach apparatus (plant viruses); blue, digestive apparatus microbiome (mycoviruses); orange, insect body (insect-specific viruses and EVEs).

The analysis of virus-derived sRNAs enabled discrimination between insect-specific viruses and associated mycoviruses, as the latter predominantly generate sRNAs with an uracil at the 5' end. On the other hand, their presence in the RNA extracts used in this study is lower, as the number of reads is less than 500 at any point in their genome, while insect-specific viruses, with the exception of TeTLV, have higher coverage (Fig. S4). Based on sRNA profiles, coverage depth, and sequence homology, TeNLV, TeTLV, TeSLV, TePLV, TeFLV, TeToLV1, and TeToLV2 are inferred to be insect-specific, while TeAAV, TeAPV1, TeAPV2, and TeABV are mycoviruses associated with their gut microbiome (Fig. 3).

Comparison with viruses reported in *D. citri* reveals substantial overlap in viral families such as *Narnaviridae*, *Totiviridae*, *Flaviviridae*, *Botourmiaviridae*, and *Partitiviridae* (Nouri et al., 2016; Matsumura et al., 2016; Lin et al., 2023; Etebari et al., 2025), indicating partial convergence of virome composition between these two psyllid species, with the exception of TeSLV and TePLV belonging to the *Solemoviridae* and *Phe-nuiviridae* families, which include species widely described in insects (Shi et al., 2016; Sun et al., 2022). In addition, we have identified two members of the *Tombusviridae* family, TeToLV1 and TeToLV2, the latter being bisegmented and with a very high homology to the unclassified *Diaphorina citri* associated C virus (Nouri et al., 2016) capable of infecting *D. citri* cell cultures (Wu et al., 2025). A separate case is that of TeAAV, which we have classified as belonging to the proposed family *Ambiguiviridae* (although not yet accepted by ICTV), whose members have only been described in fungi and whose RdRps show similarities to those of the family *Tombusviridae* (Gilbert et al., 2019; Jia et al., 2023).

It is worth noting that *T. erytrae* populations in continental Europe, including the Canary Islands and Madeira, appear largely virus-free, with the exception for TeNLV. In contrast, greater viral diversity was observed in populations from São Tomé and Príncipe and in South Africa, where the insect has been established for a longer period. Phylogenetic analyses of RdRps indicate a similarity in the amino acid sequences of TeNLVs detected in Europe compared to other locations (Fig. S6), suggesting, as in the mitochondrial genomic analysis described in Chumienti et al., 2025, a common origin in insects that have been introduced and dispersed throughout Europe. In turn, the analysis of TeNLV, TeSLV, TeToLV1, and TeToLV2 indicates a greater similarity between the sequences from Stellenbosch and Buffeljagsrivier compared to those from Gqeberha, which are more closely grouped with those from Réunion and São Tomé and Príncipe (Fig. S6) strongly suggesting regional clustering among African and island populations, reflecting historical dispersal and diversification patterns.

In summary, in this work we show the first description of the *T. erytrae* virome revealing a complex scenario in which insect-specific viruses (ISV), mycoviruses, EVEs and viruses of plant origin have been detected. ISVs can ideally be used as biocontrol agents either as bio-pesticides and/or as 'bullets' to interfere with insect vector transmission of pathogens. If any of the identified viruses were to be developed as viral vectors, the absence of corresponding EVEs or infections in European populations could confer a degree of susceptibility. The relative lack of viruses in European populations may inform future strategies for vector-targeted viral biocontrol.

Author contributions

PS, RF and VP conceived the study; AF, JAP, BR, HD, HM and RB collected samples and contributed to the experimental design; HM and RB tested samples; PS, MP, MC and VN performed bioinformatics analysis; PS, BN, FDS, LP contributed to the experimental design and provided experimental guidance; PS and VP drafted the manuscript. All the authors approved the final manuscript.

Data availability

The raw sequence data and bacterial draft genomes reported in this

paper have been deposited in the Sequence Read Archive in National Center for Biotechnology information (Accession numbers from SAMN49798494 to SAMN49798507). The data will be released upon manuscript acceptance for publication.

Impact statement

This study reveals an unprecedented diversity of actively expressed endogenous viral elements and novel insect-specific RNA viruses in *Trioza erytrae*, significantly expanding the known virosphere of psyllids and shedding light on virus-host interactions in non-model insect vectors.

Through a geographically broad metagenomic analysis, this work reveals an unexpectedly diverse virome in *Trioza erytrae*, including insect-specific viruses, mycoviruses, and actively expressed EVEs, thereby expanding the known virosphere of hemipteran insects.

Funding

This project has received funding from grants PROMETEO/CIPROM/2022/031 from the Generalitat Valenciana and the European Union's Horizon 2020 research and innovation program under grant agreement No 817,526 (PRE-HLB: Preventing HLB epidemics for ensuring citrus survival in Europe. H2020-SFS-2018-2 Topic SFS-05-2018-2019-2020-new and emerging risks to plant health). This article reflects only the authors' views, and the Agency is not responsible for any use that may be made of the information it contains.

Additional file: sequences in fasta format of the scaffolds that include new viral sequences identified in this work. Additional file 2: sequences in fasta format of the scaffolds that include fungal sequences identified in samples from São Tomé and Príncipe.

Declaration of competing interest

The authors declare that they have no known competing financial interests or personal relationships that could have appeared to influence the work reported in this paper.

Acknowledgements

The authors are grateful to Mi clay Carvalho (University of São Tomé and Príncipe), Glynnis Cook and Wayne Kirkman (Citrus Research International) for the help in collecting *T. erytrae* samples. We acknowledge to Madelein Dippenaar the artwork made for Fig. 3.

Supplementary materials

Supplementary material associated with this article can be found, in the online version, at doi:10.1016/j.virusres.2026.199710.

References

- Alqu ezar, B., Carmona, L., Bennici, S., Miranda, M.P., Bassanezi, R.B., Pe a, L., 2022. Cultural Management of Huanglongbing: current Status and Ongoing Research. *Phytopathology* 112 (1), 11–25. <https://doi.org/10.1094/PHYTO-08-21-0358-1A>.
- Arenas-Arenas, F.J., Duran-Vila, N., Quinto, J., Hervalejo,  , 2018. Is the presence of *Trioza erytrae*, vector of huanglongbing disease, endangering the Mediterranean citrus industry? Survey of its population density and geographical spread over the last years. *J. Plant Pathol.* 100, 567–574. <https://doi.org/10.1007/s42161-018-0109-8>.
- Arenas-Arenas, F.J., Duran-Vila, N., Quinto, J., Hervalejo,  , 2019. Geographic spread and inter-annual evolution of populations of *Trioza erytrae* in the Iberian Peninsula. *J. Plant Pathol.* 101, 1151–1157. <https://doi.org/10.1007/s42161-019-00301-x>.
- Britt, K., Gebben, S., Levy, A., Al, R.M., Batuman, O., 2020. The detection and surveillance of Asian citrus psyllid (*diaphorina citri*)-associated viruses in Florida citrus groves. *Front. Plant Sci.* 10, 1687. <http://doi.org/10.3389/fpls.2019.01687>.
- Britt-Ugarte mendia, K., Stevens, K., Al Rwahnih, M., Levy, A., Batuman, O., 2025. RNA-sequencing-based virome discovery in florida citrus pests. *Phytopathology*. <https://doi.org/10.1094/PBIOMES-05-24-0055-FI>.

- Bové, J.M., 2006. Huanglongbing: a destructive, new-emerging, century-old disease of citrus. *J. Plant. Pathol.* 88, 7–37.
- Carvalho, J.P., Aguiar, A.M.F., 1997. Pragas dos citrinos na Ilha da madeira. *funchal. região autónoma da madeira. secretaria regional de agricultura florestas e pescas. Direcção Regional de Agric.* 410.
- Cerqueira de Araujo, A., Huguett, E., Herniou, E.A., Drezén, J.M., Josse, T., 2022. Transposable element repression using piRNAs, and its relevance to endogenous viral elements (EVEs) and immunity in insects. *Curr. Opin. Insect Sci.* 50, 100876. <https://doi.org/10.1016/j.cois.2022.100876>.
- Couto, R.D.S., Ramos, E.D.S.F., Abreu, W.U., Rodrigues, L.R.R., Marinho, L.F., Morais, V. D.S., Villanova, F., Pandey, R.P., Deng, X., Delwart, E., et al., 2024. Metagenomic of liver tissue identified at least two genera of totivirus-like viruses in molossus molossus bats. *Microorganisms* 12, 206. <https://doi.org/10.3390/microorganisms12010206>.
- Chen, Q., Wei, T., 2020. Cell biology during infection of plant viruses in insect vectors and plant hosts. *Mol. Plant Microbe Interact.* 33 (1), 18–25. <https://doi.org/10.1094/MPMI-07-19-0184-CR>.
- Chen L., Liu Y., Wu F., Zhang J., Cui X., Wu S., Deng X., Xu M. (2023). *Citrus tristeza virus* promotes the acquisition and transmission of 'candidatus liberibacter asiaticus' by *diaphorina*. *Viruses* 15 (4):918. doi: 10.3390/v15040918.
- Chiumenti, M., Nicoloso, V., Fereres, F., Pereira, J.A., Maree, H.J., Bester, R., Reynaud, B., Delatte, H., Peña, L., Pallás, L., Serra, P., Navarro, B., Di Serio, F., 2025. Assessment of trioxa erytraea microbiome and mitochondrial genome variability by integrated high-throughput sequencing approach. *J. Pest. Sci.* 98, 2383–2402. <https://doi.org/10.1007/s10340-025-01945-8>.
- da Graça, J.V., Cook, G., Ajene, L.J., Grout, T.G., Pietersen, G., Roberts, R., Bester, R., Pretorius, M.C., Maree, H.J., 2022. A review of the 'candidatus liberibacter africanus' citrus pathosystem in Africa. focus issue: liberibacter pathosystems. *Phytopathology* 112 (1), 44–54. <https://doi.org/10.1094/PHYTO-07-21-0296-FI>.
- da Graça, J.V., Douhan, G.W., Halbert, S.E., Keremane, M.L., Lee, R.F., Vidalakis, G., Zhao, H., 2016. Huanglongbing: an overview of a complex pathosystem ravaging the world's citrus. *J. Integr. Plant Biol.* 58 (4), 373–387. <https://doi.org/10.1111/jipb.12437>.
- Danecek, P., Bonfield, J.K., Liddle, J., Marshall, J., Ohan, V., Pollard, M.O., Whitwham, A., Keane, T., McCarthy, S.A., Davies, R.M., Li, H., 2021. Twelve years of SAMtools and BCFTools. *Gigascience* 10 (2), 008 [33590861].
- de Godoy Gasparoto, M.C., Primiano, I.V., Bassanezi, R.B., Lourenço, S.A., Montesino, L. H., Wulff, N.A., Martins, E.C., Filho, A.B., Amorim, L., 2022. Prevalent transmission of 'candidatus liberibacter asiaticus' over 'ca. liberibacter americanus' in a long-term controlled environment. *Phytopathology* 112 (1), 180. <https://doi.org/10.1094/PHYTO-06-21-0239-FI>.
- Donaire, L., Ayllón, M.A., 2017. Deep sequencing of mycovirus-derived small RNAs from *Botrytis* species. *Mol. Plant Pathol.* 18 (8), 1127–1137. <https://doi.org/10.1111/mpp.12466>.
- Du, D., Kuanga, Y., Jiang, Y., Wang, Y., Cao, M., Huang, A., 2026. Complete genome characterization of *Diaphorina citri* picorna-like virus from China and a proposal for the new family *Psylloidiviridae*. *J. Invertebr. Pathol.* 216, 108562.
- Duvaud, S., Gabella, C., Lisacek, F., Stockinger, H., Ioannidis, V., Durinx, C., 2021. Expaty, the Swiss Bioinformatics Resource Portal, as designed by its users. *Nucleic. Acids. Res.* 49 (2), 216–227. <https://doi.org/10.1093/nar/gkab225>.
- Edgar, R.C., Taylor, B., Lin, V., Altman, T., Barbera, P., Melesko, D., Lohr, D., Novakovsky, G., Buchfink, B., Al-Shayeb, B., Banfield, J.F., de la Peña, M., Korobeynikov, A., Chikhi, R., Babaian, A., 2022. Petabase-scale sequence alignment catalyses viral discovery. *Nature* 602 (7895), 142–147. <https://doi.org/10.1038/s41586-021-04332-2>.
- EPO (2025) EPO global database. <https://gd.eppo.int/>.
- Etebari, K., Tugaga, A.M., Divekar, G., Ueelse, O.A., Tusa, S.S.A., Vaega, E., Sasulu, H., Uini, L., Ren, Y., Furlong, M.J., 2025. Characterising the associated virome and microbiota of asian citrus psyllid (*diaphorina citri*) in samoa. *Pathogens* 10 (8), 801. <https://doi.org/10.3390/pathogens10080801>.
- Forgia, M., Navarro, B., Daghino, S., Cervera, A., Gisel, A., Perotto, S., Aghayeva, D.N., Akinyiwa, M.F., Gobbi, E., Zheludev, I.N., Edgar, R.C., Chikhi, R., Turina, M., Babaian, A., Di Serio, F., de la Peña, M., 2023. Hybrids of RNA viruses and viroid-like elements replicate in fungi. *Nat. Commun.* 5 (1), 2591. <https://doi.org/10.1038/s41467-023-38301-2>.
- Galdeano, D.M., Rawat, T., Ingram, W., Carlson, C.R., Rodrigues Alves, G., Kuo, Y.W. (2025). Biological properties and vector competence of *Diaphorina citri* for *Candidatus Liberibacter asiaticus* modulated by an insect-specific virus. *iScience*, Vol.28 (8), p. 112982. DOI: 10.1016/j.isci.2025.112982.
- Gilbert, K.B., Holcomb, E.E., Allscheid, R.L., Carrington, J.C., 2019. Hiding in plain sight: new virus genomes discovered via a systematic analysis of fungal public transcriptomes. *PLoS. One* 14, e0219207. <https://doi.org/10.1371/journal.pone.0219207>.
- Gilbert, C., Belliardo, C., 2022. The diversity of endogenous viral elements in insects. *Curr. Opin. Insect Sci.* 49, 48–55. <https://doi.org/10.1016/j.cois.2021.11.007>.
- Goertz, G.P., Miesen, P., Overheul, G.J., van Rij, R.P., van Oers, M.M., Pijlman, G.P., 2019. Mosquito small RNA responses to west Nile and insect-specific virus infections in aedes and culex mosquito cells. *Viruses* 11 (3), 271. <https://doi.org/10.3390/v11030271>.
- González-Hernández, A., 2003. *Trioxa erytraea* (Del Guercio 1918): nueva plaga de los cítricos en canarias. *Phytoma España* 153, 112–117.
- Han, M.V., Zmasek, C.M., 2009. PhyloXML: XML for evolutionary biology and comparative genomics. *BMC. Bioinform.* 10, 356. <https://doi.org/10.1186/1471-2105-10-356>.
- Jia, J., Chen, X., Wang, X., Liu, X., Zhang, N., Zhang, B., Chang, Y., Mu, F., 2023. Molecular characterization of a novel ambivirus isolated from the phytopathogenic fungus *Setosphaeria turcica*. *Arch. Virol.* 168 (8), 199. <https://doi.org/10.1007/s00705-023-05829-z>.
- Katoh, K., Rozewicki, J., Yamada, K.D., 2019. MAFFT online service: multiple sequence alignment, interactive sequence choice and visualization. *Brief. Bioinform.* 20, 1160–1166. <https://doi.org/10.1093/bib/bbx108>. Volume.
- A.C. Leal, E., Ribeiro, D.A., Monteiro, E.S., Pantoja-Marques, F.J.C., dos Santos Mendes, J., Morais, D., Araújo, V.S., Pandey, E.L.L., Chang, R.P., Deng, C.M., Delwart, X., da Costa, E., Lima, A., 2023. *Aedes aegypti* Totivirus identified in mosquitoes in the Brazilian Amazon region. *Viruses* 59, 167–172. <https://doi.org/10.1007/s11262-022-01955-z>.
- Li, H., Durbin, R., 2010. Fast and accurate long-read alignment with burrows-wheeler transform. *Bioinformatics*. 26, 589–595 [PMID: 20080505].
- Lin C.Y., Batuman O., Levy A. (2023) Identifying the gut virome of diaphorina citri from florida groves. *insects*. 2023 Feb 8;14 (2):166. doi: 10.3390/insects14020166.
- Lin, C.Y., Buritica, J.R., Sarkar, P., Jassar, O., Vieira Rocha, S., Batuman, O., Stelinski, L. L., Levy, A., 2025. An insect virus differentially alters gene expression among life stages of an insect vector and enhances bacterial phytopathogen transmission. *J. Virol.* 99 (1). <https://doi.org/10.1128/jvi.01630-24>.
- Madeira, F., Madhusoodanan, N., Lee, J., Eusebi, A., Niewielska, A., Tivey, A.R.N., Lopez, R., Butcher, S., 2024. The EMBL-EBI Job Dispatcher sequence analysis tools framework in 2024. *Nucleic. Acids. Res.* 52 (W1), 521–525. <https://doi.org/10.1093/nar/gkae241>.
- Matsumura, E.E., Nerva, L., Nigg, J.C., Falk, B.W., Nouri, S., 2016. Complete genome sequence of the largest known flavi-like virus, *diaphorina citri* flavi-like virus, a novel virus of the asian citrus psyllid, *diaphorina citri*. *Genome Announc.* 4 (5), e00946. <https://doi.org/10.1128/genomeA.00946-16>.
- Nawrocki, E.P., Eddy, S.R., 2013. *infernal 1.1: 100-fold faster RNA homology searches*. *Bioinformatics* 29, 2933–2935.
- Nigg, J.C., Kuo, Y.W., Falk, B.W., 2020. Endogenous viral element-derived piwi-interacting RNAs (piRNAs) are not required for production of ping-pong-dependent piRNAs from *Diaphorina citri* densovirus. *mBio* 11, 02209–02220. <https://doi.org/10.1128/mBio.02209-20>.
- Nouri, S., Salem, N., Falk, B.W., 2016. Complete genome sequence of *diaphorina citri*-associated C virus, a novel putative RNA virus of the Asian citrus psyllid, *diaphorina citri*. *Genome Announc.* 4 (4), e00639. <https://doi.org/10.1128/genomeA.00639-16>.
- Nouri, S., Matsumura, E.E., Kuo, Y.W., Falk, B.W., 2018. Insect-specific viruses: from discovery to potential translational applications. *Curr. Opin. Virol.* 33, 33–41.
- Pang, T., Peng, J., Bian, R., Liu, Y., Zhang, D., Andika, I.B., Sun, L., 2022. Similar characteristics of siRNAs of plant viruses which replicate in plant and fungal hosts. *Biology* 17 (11), 1672. <https://doi.org/10.3390/biology11111672>.
- Pérez-Otero, R., Mansilla, J.P., del Estal, P., 2015. Detección de la psila africana de los cítricos, *trioxa erytraea* (del guercio, 1918) (hemiptera: psylloidea: trioziidae), en la península ibérica. *Archivos Entomológicos* 13, 119–122.
- Rashidi, M., Lin, C.Y., Britt, K., Batuman, O., Al Rwahnih, M., Achor, D., Levy, A., 2022. *Diaphorina citri* flavi-like virus localization, transmission, and association with *candidatus liberibacter asiaticus* in its psyllid host. *Virology* 567, 47–56. <https://doi.org/10.1016/j.virol.2021.12.009>.
- Reynaud, B., Turpin, P., Molinari, F.M., Grondin, M., Roque, S., Chiroleu, F., Fereres, A., Delatte, H., 2022. The African citrus psyllid *trioxa erytraea*: an efficient vector of *candidatus liberibacter asiaticus*. *Front. Plant Sci.* 22 (13), 1089762. <https://doi.org/10.3389/fpls.2022.1089762>.
- Rufz-Rivero, O., Garcia-Lor, A., Rojas-Panadero, B., Franco, J.C., Khamis, F.M., Kruger, K., Cifuentes, D., Bielza, P., Tena, A., Urbaneja, A., Pérez-Hedo, M., 2021. Insights into the origin of the invasive populations of *Trioxa erytraea* in Europe using microsatellite markers and mtDNA barcoding approaches. *Sci. Rep.* 11 (1), 18651. <https://doi.org/10.1038/s41598-021-97824-0>.
- Shi, M., Lin, X.D., Tian, J.H., Chen, L.J., Chen, X., Li, C.X., Qin, X.C., Li, J., Cao, J.P., Eden, J. S., Buchmann, J., Wang, W., Xu, J., Holmes, E.C., Zhang, Y.Z., 2016. Redefining the invertebrate RNA virosphere. *Nature* 540 (7634), 539–543. <https://doi.org/10.1038/nature20167>.
- Sun, M.H., Ji, Y.F., Li, G.H., Shao, J.W., Chen, R.X., Gong, H.Y., Chen, S.Y., Chen, J.M., 2022. Highly adaptive *Phenuiviridae* with biomedical importance in multiple fields. *J. Med. Virol.* 94 (6), 2388–2401. <https://doi.org/10.1002/jmv.27618>.
- Tekpinar, A.D., Kalmer, A., 2019. Utility of various molecular markers in fungal identification and phylogeny. *Nova Hedwigia* 109, 187–224. https://doi.org/10.1127/nova_hedwigia/2019/0528.
- ter Horst, A.M., Nigg, J.C., Dekker, F.M., Falk, B.W., 2019. Endogenous viral elements are widespread in arthropod genomes and commonly give rise to PIWI-interacting RNAs. *J. Virol.* 93, e02124. <https://doi.org/10.1128/JVI.02124-18>.
- Valles, S.M., Rivers, A.R., 2019. Nine new RNA viruses associated with the fire ant *solenopsis invicta* from its native range. *Viruses* 55, 368–380. <https://doi.org/10.1007/s11262-019-01652-413>.
- Wang, N., Pierson, E.A., Setubal, J.C., Xu, J., Levy, J.G., Zhang, Y., Li, J., Rangel, L.T., Jr, M. J., 2017. The *candidatus liberibacter*-host interface: insights into pathogenesis mechanisms and disease control. *Annu Rev. Phytopathol.* 55, 451–482. <https://doi.org/10.1146/annurev-phyto-080516-035513>.
- Wang, S., Li, P., Zhang, J., Qiu, D., Guo, L., 2016. Generation of a high resolution map of sRNAs from *fusarium graminearum* and analysis of responses to viral infection. *Sci. Rep.* 6, 26151. <https://doi.org/10.1038/srep26151>.
- Wang, Q., Cheng, S., Xiao, X., Cheng, J., Fu, Y., Chen, T., Jiang, D., Xie, J., 2019. Discovery of two mycoviruses by high-throughput sequencing and assembly of mycovirus-derived small silencing RNAs from a hypovirulent strain of *sclerotinia*

- sclerotiorum*. Front. Microbiol. 10, 1415. <https://doi.org/10.3389/fmicb.2019.01415>.
- Wu, F., Huang, M., Fox, E.GP., Huang, J., Cen, Y., Deng, X., Xu, M., 2021. Preliminary report on the acquisition, persistence and potential transmission of *citrus tristeza virus* by *diaphorina citri*. Insects 12 (8), 735. <https://doi.org/10.3390/insects12080735>.
- Wu, K., Vu, E.D, Ghosh, S., Mishra, R., Bonning, B.C., 2025. Continuous cell lines derived from the Asian citrus psyllid, *diaphorina citri*, harbor viruses and wolbachia. Sci. Rep. 15 (1), 124. <https://doi.org/10.1038/s41598-024-83671-2>.